Composite Materials and Engineering, *Vol. 3, No. 1 (2021) 25-40*
DOI: https://doi.org/10.12989/cme.2021.3.1.025

Effect of porosity on fundamental frequencies of FGM sandwich plates

Rabia Benferhat, Tahar Hassaine Daouadji* and Rabahi Abderezak

Laboratory of Geomatics and Sustainable Development, University of Tiaret, Algeria

(Received March 9, 2020, Revised September 11, 2020, Accepted September 16, 2020)

Abstract. In this paper, the porosities effect on the dynamic analysis of the simply supported FGM sandwich plates is studied using a new refined shear deformation theory taking into account transverse shear deformation effects. This porosity may possibly occur inside the Functionally Graded Materials (FGMs) during their fabrication. Two common types of FGM sandwich plates are considered, namely, the sandwich with the FGM face sheet and the homogeneous core and the sandwich with the homogeneous face sheet and the FGM core. The results are presented for two constituent metal-ceramic functionally graded plates that have a power law through-the-thickness variation of the volume fractions of the constituents. The results obtained reveal that the dynamic response is significantly influenced by the volume fraction of the porosity, power law index, the thickness-side ratios and the thickness of the functionally graded layer.

Keywords: FGM sandwich plates; dynamic response; refined plate theory; porosity

1. Introduction

Functionally Graded Materials (FGMs) are microscopically inhomogeneous composites that are usually made from a mixture of metals and ceramics. FGMs are regarded as one of the most promising candidates for future advanced composites in many engineering sectors such as the aerospace, aircraft, automobile and defense industries, and most recently the electronics and biomedical sectors (Ichikawa 2000).

The term FGMs was originated in the mid-1980s by a group of scientists in Japan; where this new material concept was proposed to increase adhesion and minimize the thermal stresses. Since then, an effort to develop high-resistant materials using FGMs had been continued. FGMs have the properties that could vary in several suitable directions (Koizumi 1997, Benferhat *et al*. 2016b). The mechanical properties of these materials are often being represented in the form of a series (Shi and Chen 2004) and power-law index variations (Hassaine *et al*. 2016a, Abdelhak *et al*. 2016b, Adim and Hassaine 2016, Daouadji and Benferhat 2016, Abdedezak *et al*. 2016b, 2018, Adim *et al*. 2018, Benhenni *et al*. 2019a, b, Hadj *et al*. 2019, Hassaine Daouadji 2013, Belkacem 2016a). In these graded materials, there is a smooth and continuous variation of material properties across the thickness. This leads to no stress concentration and better fatigue life.

Sandwich structures are often found in aerospace application such as in skin of wings, vertical

*Corresponding author, Professor, E-mail: daouadjitahar@gmail.com

http://www.techno-press.org/?journal=cme&subpage=7 ISSN: 2671-4930 (Print), 2671-5120 (Online)

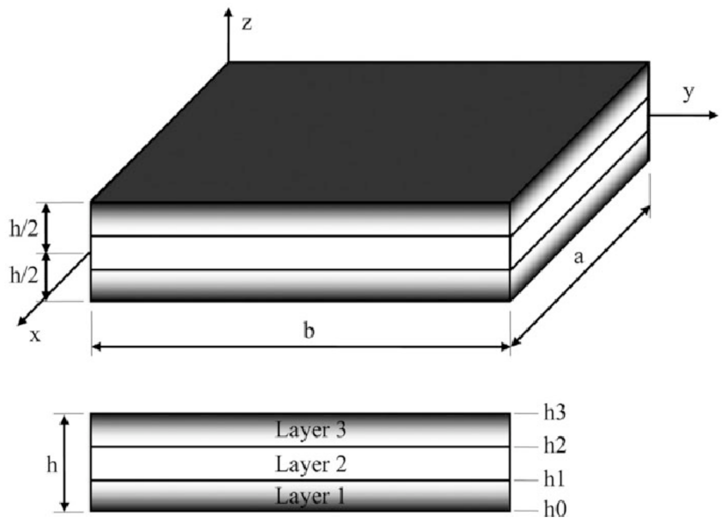

Fig. 1 The geometry of FGM sandwich plate

fin torque box, aileron, spoilers, etc. The advantages of these structures are that it provides high specific stiffness and strength for a low-weight consideration. To maintain minimum weight for a given thermo-mechanical loading condition, FGM could be incorporated in the sandwich construction (Pradhan and Murmu 2009, Rabia *et al*. 2016b, 2018b, Benhenni *et al*. 2018, Belkacem *et al*. 2016b, Hassaine Daouadji 2016c, Rabahi 2019, Adim 2016). However, the literature on the analysis of the FGMs sandwich plate is very few. Zenkour and Sobhy (2010) studied the thermal buckling of functionally graded material sandwich plates. The thermal loads are assumed to be uniform, linear and non-linear distribution through-the-thickness. Wang and Shen (2011) carried out nonlinear vibration, nonlinear bending and post-buckling analyses for a sandwich plate with FGM face sheets resting on an elastic foundation in thermal environments. Natarajan and Manickam (2012) carried out the bending and the free flexural vibration behavior of sandwich FGM plates using an accurate theory which take accounts for the realistic variation of the displacements through the thickness.

However, in FGM fabrication, micro voids or porosities can occur within the materials during the process of sintering. This is because of the large difference in solidification temperatures between material constituents (Zhu *et al*. 2000, Daouadji and Adim 2016a, b, Rabahi *et al*. 2016a, 2019). Wattanasakulpong and Ungbhakorn (2014) also gave the discussion on porosities happening inside FGM samples fabricated by a multi-step sequential infiltration technique. Therefore, it is important to take in to account the porosity effect when designing FGM structures subjected to dynamic loadings. Recently, Wattanasakulpong and Ungbhakorn (2014) studied linear and nonlinear vibration problems of elastically and restrained FG beams having porosities.

2. Geometric configuration and material properties

2.1 Geometric configuration

Fig. 1 shows rectangular FGM sandwich plate with the uniform thickness composed of three

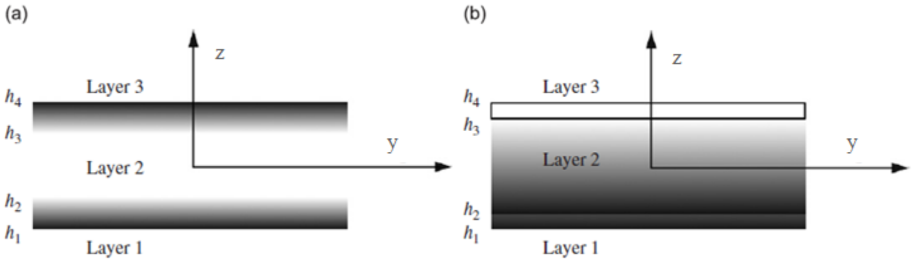

(a) FGM facesheet and homogeneous core (b) homogeneous facesheet and FGM core.

Fig. 2 The material variation along the thickness of the FGM sandwich plate

microscopically heterogeneous layers under consideration and the Cartesian coordinate system (*x*, *y*, *z*) used in the present study. The modified rule of mixture covering porosity phases is used to describe and approximate material properties of the FG sandwich plates (Fig. 2).

2.2 Numerical simulation procedure

Two different types of functionally graded plates are studied (Hadji *et al*. 2015, Hassaine Daouadji *et al*. 2016b, Rabahi *et al*. 2018a).

Type A: Power-law FGM face sheet and homogeneous core

$$V^{(1)} = \left(\frac{z-h_1}{h_2-h_1}\right)^k, \qquad z \in [h_1, h_2]$$
$$V^{(2)} = 1, \qquad z \in [h_2, h_3] \tag{1}$$
$$V^{(3)} = \left(\frac{z-h_4}{h_3-h_4}\right)^k, \qquad z \in [h_3, h_4]$$

Type B: Homogeneous face sheet and power-law FGM core

$$V^{(1)} = 0, \qquad z \in [h_1, h_2]$$
$$V^{(2)} = \left(\frac{z-h_2}{h_3-h_2}\right)^k, \qquad z \in [h_2, h_3] \tag{2}$$
$$V^{(3)} = 1, \qquad z \in [h_3, h_4]$$

where $V(n)$ (n = 1, 2, 3) denote the volume fraction function of layer n and k is the volume fraction index ($0 \leq k \leq \infty$), which dictates the material variation profile through the thickness.

2.3 Effective material properties FGM sandwich plates

A FG plate made from a mixture of two material phases, for example, a metal and a ceramic. The material properties of FG plates are assumed to vary continuously through the thickness of the plate. In this investigation, the imperfect plate is assumed to have porosities spreading within the thickness due to defect during production. Consider an imperfect FGM with a porosity volume fraction, α ($\alpha \ll 1$), distributed evenly among the metal and ceramic, the modified rule of mixture proposed by Wattanasakulpong and Ungbhakorn (2014) is used as

$$P = P_m(V_m - \frac{\alpha}{2}) + P_c(V_c - \frac{\alpha}{2}) \tag{3}$$

Now, the total volume fraction of the metal and ceramic is: $V_m + V_c = 1$, and the power law of volume fraction of the ceramic is described as

$$V_c = (\frac{z}{h} + \frac{1}{2})^k \tag{4}$$

Hence, all properties of the imperfect FGM can be written as

$$P = (P_c - P_m)(\frac{z}{h} + \frac{1}{2})^k + P_m - (P_c + P_m)\frac{\alpha}{2} \tag{5}$$

It is noted that the positive real number k ($0 \le k \le \infty$), is the power law or volume fraction index, and z is the distance from the mid-plane of the FG plate. The FG plate becomes a fully ceramic plate when k is set to zero and fully metal for large value of k. Thus, the Young's modulus (E) and material density (ρ) equations of the imperfect FGM beam can be expressed as (Atmane *et al*. 2015, Hadji *et al*. 2015, Hassaine Daouadji 2017, Daouadji *et al*. 2008)

$$\begin{aligned} E(z) &= (E_c - E_m)(\frac{z}{h} + \frac{1}{2})^k + E_m - (E_c + E_m)\frac{\alpha}{2} \\ \rho(z) &= (\rho_c - \rho_m)(\frac{z}{h} + \frac{1}{2})^k + \rho_m - (\rho_c + \rho_m)\frac{\alpha}{2} \end{aligned} \tag{6}$$

However, Poisson's ratio (v) is assumed to be constant. The material properties of a perfect FG plate can be obtained when α is set to zero.

3. Mathematical formulation

The displacements of a material point located at (x, y, z) in the plate may be written as follows

$$\begin{cases} u(x,y,z) = u_0(x,y) - z\dfrac{\partial w_b}{\partial x} - (z - \sin(\dfrac{\pi z}{h}))\dfrac{\partial w_s}{\partial x} \\ v(x,y,z) = v_0(x,y) - z\dfrac{\partial w_b}{\partial y} - (z - \sin(\dfrac{\pi z}{h}))\dfrac{\partial w_s}{\partial y} \\ w(x,y,z) = w_b(x,y) + w_s(x,y) \end{cases} \tag{7}$$

where u_0 and v_0 are the mid-plane displacements of the plate in the x and y direction, respectively; w_b and w_s are the bending and shear components of transverse displacement, respectively, while $f(z)$ represents shape functions determining the distribution of the transverse shear strains and stresses along the thickness and is given as (Benferhat *et al*. 2016a, Rabia *et al*. 2016c)

$$f(z) = z - \sin(\frac{\pi z}{h}) \tag{8}$$

The strain components are related to the displacements given in Eq. (7) can be expressed as

$$\begin{aligned} \varepsilon_x &= \varepsilon_x^0 + z\,k_x^b + (z - \sin(\frac{\pi z}{h}))k_x^s \\ \varepsilon_y &= \varepsilon_y^0 + z\,k_y^b + (z - \sin(\frac{\pi z}{h}))\,k_y^s \end{aligned} \tag{9}$$

$$\begin{aligned}
\gamma_{xy} &= \gamma_{xy}^{0} + z\,k_{xy}^{b} + (z - \sin(\frac{\pi z}{h}))\,k_{xy}^{s} \\
\gamma_{yz} &= g(z)\,\gamma_{yz}^{s} = (1 - \frac{d(z - \sin(\frac{\pi z}{h}))}{dz})\,\gamma_{yz}^{s} \\
\gamma_{xz} &= g(z)\,\gamma_{xz}^{s} = (1 - \frac{d(z - \sin(\frac{\pi z}{h}))}{dz})\,\gamma_{xz}^{s} \\
\varepsilon_{z} &= 0
\end{aligned} \tag{9}$$

where

$$\begin{aligned}
&\varepsilon_{x}^{0} = \frac{\partial u_0}{\partial x}, \quad k_{x}^{b} = -\frac{\partial^2 w_b}{\partial x^2}, \quad k_{x}^{s} = -\frac{\partial^2 w_s}{\partial x^2} \\
&\varepsilon_{y}^{0} = \frac{\partial v_0}{\partial y}, \quad k_{y}^{b} = -\frac{\partial^2 w_b}{\partial y^2}, \quad k_{y}^{s} = -\frac{\partial^2 w_s}{\partial y^2}, \\
&\gamma_{xy}^{0} = \frac{\partial u_0}{\partial y} + \frac{\partial v_0}{\partial x}, \quad k_{xy}^{b} = -2\frac{\partial^2 w_b}{\partial x \partial y}, \quad k_{xy}^{s} = -2\frac{\partial^2 w_s}{\partial x \partial y}, \quad \gamma_{yz}^{s} = \frac{\partial w_s}{\partial y} \\
&\gamma_{xz}^{s} = \frac{\partial w_s}{\partial x}, \quad f'(z) = \frac{df(z)}{dz} = \frac{d(z - \sin(\frac{\pi z}{h}))}{dz} \\
&g(z) = 1 - f'(z) = 1 - \frac{d(z - \sin(\frac{\pi z}{h}))}{dz}
\end{aligned} \tag{10}$$

The stress-strain relationships accounting for transverse shear deformation in the plate coordinate can be written as

$$\begin{Bmatrix} \sigma_x \\ \sigma_y \\ \tau_{xy} \end{Bmatrix} = \begin{bmatrix} Q_{11} & Q_{12} & 0 \\ Q_{12} & Q_{22} & 0 \\ 0 & 0 & Q_{66} \end{bmatrix} \begin{Bmatrix} \varepsilon_x \\ \varepsilon_y \\ \gamma_{xy} \end{Bmatrix}$$
$$\begin{Bmatrix} \tau_{yz} \\ \tau_{zx} \end{Bmatrix} = \begin{bmatrix} Q_{44} & 0 \\ 0 & Q_{55} \end{bmatrix} \begin{Bmatrix} \gamma_{yz} \\ \gamma_{zx} \end{Bmatrix} \tag{11}$$

where (σ_x, σ_y, τ_{xy}, τ_{xz}, τ_{yz}) and (ε_x, ε_x, γ_{xy}, γ_{xz}, γ_{yz}) are the stress and strain components, respectively.

Stiffness coefficients, Q_{ij} can be expressed as

$$Q_{11} = Q_{22} = \frac{E(z)}{1 - \nu^2}, \qquad Q_{12} = \frac{\nu E(z)}{1 - \nu^2}, \qquad Q_{44} = Q_{55} = Q_{66} = \frac{E(z)}{2(1 + \nu)} \tag{12}$$

The total potential energy of the FGM sandwich plate may be written as

$$U_e = \frac{1}{2}\int_V (\sigma_x \varepsilon_x + \sigma_y \varepsilon_y + \tau_{xy}\gamma_{xy} + \tau_{yz}\gamma_{yz} + \tau_{zx}\gamma_{zx})dV \tag{13}$$

The principle of virtual work for the present problem may be expressed as follows

$$\begin{aligned}
U_e = \frac{1}{2}\int_V \big(&N_x \varepsilon_x^0 + N_y \varepsilon_y^0 + N_{xy}\varepsilon_{xy}^0 + M_x^b k_x^b + M_y^b k_y^b + M_{xy}^b k_{xy}^b + M_x^s k_x^s + M_y^s k_y^s \\
&+ M_{xy}^s k_{xy}^s + S_{yz}^s \gamma_{yz}^s + S_{xz}^s \gamma_{xz}^s\big)dxdy
\end{aligned} \tag{14}$$

where

$$\begin{Bmatrix} N_x, & N_y, & N_{xy}, \\ M_x^b, & M_y^b, & M_{xy}^b, \\ M_x^s, & M_y^s, & M_{xy}^s, \end{Bmatrix} = \int_{-\frac{h}{2}}^{+\frac{h}{2}} (\sigma_x, \sigma_y, \tau_{xy}) \begin{Bmatrix} 1 \\ z \\ f(z) \end{Bmatrix} dz \tag{15}$$

$$(S_{xz}^s, S_{yz}^s) = \int_{-\frac{h}{2}}^{+\frac{h}{2}} (\tau_{xz}, \tau_{yz})\, g(z) dz \tag{16}$$

The kinetic energy of the plate can be written as

$$\begin{aligned} T = \frac{1}{2\int_v \rho(\ddot{U}^2 + \ddot{V}^2 + \ddot{W}^2)dV} = \frac{1}{2\int_A I_0(\ddot{u}^2 + \ddot{v}^2 + (\ddot{w}_b + \ddot{w}_s)^2)dxdy} \\ + 1/2 \int_A (I_2((\frac{\partial \ddot{w}_b}{\partial x})^2 + (\frac{\partial \ddot{w}_b}{\partial y})^2) + \frac{I_2}{84}((\frac{\partial \ddot{w}_s}{\partial x})^2 + (\frac{\partial \ddot{w}_s}{\partial y})^2))dxdy \end{aligned} \tag{17}$$

where ρ is the mass of density of the FG plate and I_i (i = 0, 2) are the inertias defined by

$$(I_0, I_2) = \sum_{n=1}^{3} \int_{h_n}^{h_{n+1}} (1, z^2)\rho dz \tag{18}$$

Hamilton's principle (Delale and Erdogan 1983) is used to derive the equations of motion appropriate to the displacement field and the constitutive equation. The principle can be stated in an analytical form as

$$0 = \int_0^t \delta(U_e - T)dt \tag{19}$$

where δ indicates a variation with respect to x and y.

By substituting Eqs. (14) and (17) into Eq. (19) and integrating the equation by parts and collecting the coefficients of δu, δv, δw_b and δw_s, the equations of motion for the FG sandwich plate are obtained as follows

$$\begin{cases} \delta u: \dfrac{\partial N_x}{\partial x} + \dfrac{\partial N_{xy}}{\partial y} = I_0 \ddot{u} \\ \delta v: \dfrac{\partial N_{xy}}{\partial x} + \dfrac{\partial N_y}{\partial y} = I_0 \ddot{v} \\ \delta w_b: \dfrac{\partial^2 M_x^b}{\partial x^2} + 2\dfrac{\partial^2 M_{xy}^b}{\partial x \partial y} + \dfrac{\partial^2 M_y^b}{\partial y^2} = I_0(\ddot{w}_b + \ddot{w}_s) - I_2(\dfrac{\partial^2 \ddot{w}_b}{\partial x^2} + \dfrac{\partial^2 \ddot{w}_b}{\partial y^2}) \\ \delta w_s: \dfrac{\partial^2 M_x^s}{\partial x^2} + 2\dfrac{\partial^2 M_{xy}^s}{\partial x \partial y} + \dfrac{\partial^2 M_y^s}{\partial y^2} + \dfrac{\partial S_{xz}^s}{\partial x} + \dfrac{\partial S_{yz}^s}{\partial y} = I_0(\ddot{w}_b + \ddot{w}_s) - \dfrac{I_2}{84}(\dfrac{\partial^2 \ddot{w}_b}{\partial x^2} + \dfrac{\partial^2 \ddot{w}_b}{\partial y^2}) \end{cases} \tag{20}$$

Using Eq. (11) in Eq. (15), the stress resultants of a sandwich plate made up of three layers can be related to the total strains by

$$\begin{Bmatrix} N \\ M^b \\ M^s \end{Bmatrix} = \begin{bmatrix} A & B & B^s \\ A & D & D^s \\ B^s & D^s & H^s \end{bmatrix} \begin{Bmatrix} \varepsilon \\ k^b \\ k^s \end{Bmatrix}, \qquad S = A^s \gamma \tag{21}$$

Table 1 Fundamental frequency results for FGM sandwich plate with homogeneous hardcore

h/b	k	Theory	ω						
			α	1-0-1	2-1-2	1-1-1	2-2-1	1-2-1	1-8-1
0.01	0	Li *et al.* (2008)	α =0	1.88829	1.88829	1.88829	1.88829	1.88829	1.88829
		Present	α = 0	1.88825	1 .88825	1.88825	1.88825	1.88825	1.88825
			α = 0.1	1.97464	1.95642	1.94455	1.93869	1.93001	1.90463
			α = 0.2	2.07409	2.03256	2.00621	1.99341	1.97467	1.92145
	5	Li *et al.* (2008)	α = 0	0.96563	0.99903	1.06309	1.13020	1.19699	1.56988
		Present	α = 0	0.96564	0.99904	1.06309	1.13019	1.19697	1.56985
			α = 0.1	1.02506	1.04426	1.10114	1.16570	1.22718	1.58416
			α = 0.2	1.09700	1.09624	1.14361	1.20478	1.25981	1.59888
	10	Li *et al.* (2008)	α = 0	0.95042	0.95934	1.01237	1.08065	1.14408	1.54164
		Present	α = 0	0.95045	0.95937	1.01236	1.08068	1.14405	1.54162
			α = 0.1	1.01080	1.00382	1.04928	1.11516	1.17331	1.55362
			α = 0.2	1.08435	1.05509	1.09055	1.15320	1.20494	1.56808
0.1	0	Li *et al.* (2008)	α = 0	1.82682	1.82682	1.82682	1.82682	1.82682	1.82682
		Present	α = 0	1.82453	1.82453	1.82453	1.83453	1.82453	1.82453
			α = 0.1	1.90493	1.88882	1.87815	1.87259	1.86481	1.84065
			α = 0.2	1.99724	1.96058	1.93690	1.92474	1.90793	1.85722
	5	Li *et al.* (2008)	α = 0	0.94476	0.98103	1.04532	1.10983	1.17567	1.52993
		Present	α = 0	0.94630	0.98207	1.04481	1.10892	1.17399	1.52777
			α = 0.1	1.00262	1.02620	1.08223	1.14374	1.20386	1.54199
			α = 0.2	1.07018	1.07692	1.12401	1.18209	1.23616	1.55662
	10	Li *et al.* (2008)	α = 0	0.92727	0.94078	0.99523	1.06104	1.12466	1.50333
		Present	α = 0	0.92874	0.94326	0.99545	1.06260	1.12262	1.50121
			α = 0.1	0.98451	0.98658	1.03203	1.09493	1.15216	1.51525
			α = 0.2	1.05079	1.03655	1.07268	1.13230	1.18350	1.52971

where

$$N = \{N_x, N_y, N_{xy}\}^t, \qquad M^b = \{M_x^b, M_y^b, M_{xy}^b\}^t, \qquad M^s = \{M_x^s, M_y^s, M_{xy}^s\}^t \tag{22}$$

$$\varepsilon = \{\varepsilon_x^0, \varepsilon_y^0, \varepsilon_{xy}^0\}^t, \qquad k^b = \{k_x^b, k_y^b, k_{xy}^b\}^t, \qquad k^s = \{k_x^s, k_y^s, k_{xy}^s\}^t \tag{23}$$

$$A = \begin{bmatrix} A_{11} & A_{12} & 0 \\ A_{12} & A_{22} & 0 \\ 0 & 0 & A_{66} \end{bmatrix}, \qquad B = \begin{bmatrix} B_{11} & B_{12} & 0 \\ B_{12} & B_{22} & 0 \\ 0 & 0 & B_{66} \end{bmatrix}, \qquad D = \begin{bmatrix} D_{11} & D_{12} & 0 \\ D_{12} & D_{22} & 0 \\ 0 & 0 & D_{66} \end{bmatrix} \tag{24}$$

$$B^s = \begin{bmatrix} B_{11}^s & B_{12}^s & 0 \\ B_{12}^s & B_{22}^s & 0 \\ 0 & 0 & B_{66}^s \end{bmatrix}, \qquad D^s = \begin{bmatrix} D_{11}^s & D_{12}^s & 0 \\ D_{12}^s & D_{22}^s & 0 \\ 0 & 0 & D_{66}^s \end{bmatrix}, \qquad H^s = \begin{bmatrix} H_{11}^s & H_{12}^s & 0 \\ H_{12}^s & H_{22}^s & 0 \\ 0 & 0 & H_{66}^s \end{bmatrix} \tag{25}$$

$$S = \left\{S_{xz}^{z}, S_{yz}^{s}\right\}^{t}, \qquad \gamma = \left\{\gamma_{xz}, \gamma_{yz}\right\}^{t}, \qquad A^{s} = \begin{bmatrix} A_{44}^{s} & 0 \\ 0 & A_{55}^{s} \end{bmatrix} \tag{26}$$

The stiffness coefficients A_{ij} and B_{ij}, etc., are defined as

$$\begin{Bmatrix} A_{11} & B_{11} & D_{11} & B_{11}^{s} & D_{11}^{s} & H_{11}^{s} \\ A_{12} & B_{12} & D_{12} & B_{12}^{s} & D_{12}^{s} & H_{12}^{s} \\ A_{66} & B_{66} & D_{66} & B_{66}^{s} & D_{66}^{s} & H_{66}^{s} \end{Bmatrix} = \int_{-\frac{h}{2}}^{+\frac{h}{2}} Q_{11}\left(1, z, z^{2}, f(z), zf(z), f^{2}(z)\right) \begin{Bmatrix} 1 \\ \nu \\ \dfrac{1-\nu}{2} \end{Bmatrix} dz \tag{27}$$

$$\left(A_{22}, B_{22}, D_{22}, B_{22}^{s}, D_{22}^{s}, H_{22}^{s}\right) = \left(A_{11}, B_{11}, D_{11}, B_{11}^{s}, D_{11}^{s}, H_{11}^{s}\right) \tag{28}$$

$$A_{44}^{s} = A_{55}^{s} = \int_{-\frac{h}{2}}^{+\frac{h}{2}} \frac{E(z)}{2(1+\nu)} [g(z)]^{2} dz \tag{29}$$

$$(I_1, I_2, I_3, I_4, I_5, I_6) = \sum_{n=1}^{3} \int_{-h/2}^{h/2} \left(1, z, z^{2}, f(z), zf(z), (f(z))^{2}\right) \rho(z) dz \tag{30}$$

Eq. (20) can be expressed in terms of displacements (u, v, w_b, w_s) by substituting the stress resultants from Eq. (21). For FG plates, the equilibrium Eq. (20) take the forms

$$\begin{aligned} &A_{11}d_{11}u_0 + A_{66}D_{22}u_0 + (A_{12}+A_{66})d_{12}v_0 - B_{11}d_{11}w_b - (B_{12}+2B_{66})d_{122}w_b \\ &-(B_{12}^{s}+2B_{66}^{s})d_{122}w_s - B_{11}^{s}d_{111}w_s = I_0\ddot{u} \end{aligned} \tag{31}$$

$$\begin{aligned} &A_{22}d_{22}v_0 + A_{66}d_{11}v_0 + (A_{12}+A_{66})d_{12}u_0 - B_{22}d_{222}w_b - (B_{12}+2B_{66})d_{112}w_b \\ &-(B_{12}^{s}+2B_{66}^{s})d_{112}w_s - B_{22}^{s}d_{222}w_s = I\ddot{v} \end{aligned} \tag{32}$$

$$\begin{aligned} &B_{11}d_{111}u_0 + (B_{12}+2B_{66})d_{122}u_0 + (B_{12}+2B_{66})d_{112}v_0 + B_{22}d_{222}v_0 - D_{11}d_{1111}w_b \\ &-2(D_{12}+2D_{66})d_{1122}w_b - D_{22}d_{2222}w_b - D_{11}^{s}d_{1111}w_s - 2(D_{12}^{s}+2D_{66}^{s})d_{1122}w_s \\ &-D_{22}^{s}d_{2222}w_s = I_0(\ddot{w}_b + w_s) - I_2\nabla^{2}\ddot{w}_b \end{aligned} \tag{33}$$

$$\begin{aligned} &B_{11}^{s}d_{111}u_0 + (B_{12}^{s}+2B_{66}^{s})d_{122}u_0 + (B_{12}^{s}+2B_{66}^{s})d_{112}v_0 + B_{22}^{s}d_{222}v_0 - D_{11}^{s}d_{1111}w_b \\ &-2(D_{12}^{s}+2D_{66}^{s})d_{1122}w_b - D_{22}^{s}d_{2222}w_b - H_{11}^{s}d_{1111}w_s - 2(H_{12}^{s}+2H_{66}^{s})d_{1122}w_s \\ &-H_{22}^{s}d_{2222}w_s + A_{55}^{s}d_{11}w_s + A_{44}^{s}d_{22}w_s = I_0(\ddot{w}_b + w_s) - \frac{\ddot{I}_2}{84}\nabla^{2}\ddot{w}_b \end{aligned} \tag{34}$$

where d_{ij}, d_{ijl} and d_{ijlm} are the following differential operators

$$d_{ij} = \frac{\partial^{2}}{\partial x_i \partial x_j}, \qquad d_{ijl} = \frac{\partial^{3}}{\partial x_i \partial x_j \partial x_l}, \qquad d_{ijlm} = \frac{\partial^{4}}{\partial x_i \partial x_j \partial x_l \partial x_m}, \qquad (i, j, l, m = 1, 2) \tag{35}$$

The following representation for the displacement quantities of the shear deformation theories is appropriate in the case of the free vibration problem

$$\begin{Bmatrix} u_0 \\ v_0 \\ w_b \\ w_s \end{Bmatrix} = \sum_{m=1}^{\infty} \sum_{n=1}^{\infty} \begin{Bmatrix} U_{mn}\cos(\lambda x)\sin(\mu y)e^{i\omega t} \\ V_{mn}\sin(\lambda x)\cos(\mu y)e^{i\omega t} \\ W_{bmn}\sin(\lambda x)\sin(\mu y)e^{i\omega t} \\ W_{smn}\sin(\lambda x)\sin(\mu y)e^{i\omega t} \end{Bmatrix} \tag{36}$$

Table 2 Fundamental frequency results for perfect and imperfect FGM sandwich plate with homogeneous soft-core

h/b	k	Theory	ω						
			α	1-0-1	2-1-2	1-1-1	2-2-1	1-2-1	1-8-1
0.01	0	Li *et al.* (2008)	α =0	0.96022	0.96022	0.96022	0.96022	0.96022	0.96022
		Present	$\alpha = 0$	0.96021	0.96021	0.96021	0.96021	0.96021	0.96021
			$\alpha = 0.1$	1.02355	1.00992	1.00111	0.99678	0.99041	0.97196
			$\alpha = 0.2$	1.10114	1.06822	1.04773	1.03789	1.02366	0.98415
	5	Li *et al.* (2008)	$\alpha = 0$	1.92090	1.94313	1.93623	1.86207	1.88530	1.57035
		Present	$\alpha = 0$	1.92089	1.94329	1.93653	1.86236	1.88552	1.57035
			$\alpha = 0.1$	2.01349	2.02128	2.00310	1.92081	1.93591	1.58833
			$\alpha = 0.2$	2.12093	2.10950	2.07706	1.98514	1.99058	1.60695
	10	Li *et al.* (2008)	$\alpha = 0$	1.91064	1.94687	1.95044	1.88042	1.91162	1.60457
		Present	$\alpha = 0$	1.91061	1.94699	1.95075	1.88134	1.91190	1.60457
			$\alpha = 0.1$	2.00053	2.02358	2.01668	1.93884	1.96233	1.62299
			$\alpha = 0.2$	2.10447	2.10999	2.08978	2.00270	2.01696	1.64202
0.1	0	Li *et al.* (2008)	$\alpha = 0$	0.92897	0.92897	0.92897	0.92897	0.92897	0.92897
		Present	$\alpha = 0$	0.92780	0.92780	0.92780	0.92780	0.92780	0.92780
			$\alpha = 0.1$	0.97725	0.96995	0.96406	0.96024	0.95580	0.93930
			$\alpha = 0.2$	1.01821	1.01583	1.00439	0.99593	0.98651	0.95124
	5	Li *et al.* (2008)	$\alpha = 0$	1.841 98	1.82611	1.78956	1.72726	1.72670	1.46647
		Present	$\alpha = 0$	1.841 14	1.83869	1.81275	1.75030	1.74351	1.46626
			$\alpha = 0.1$	1.92443	1.90628	1.86905	1.80018	1.78585	1.48304
			$\alpha = 0.2$	2.02034	1.98201	1.93105	1.85464	1.83159	1.50040
	10	Li *et al.* (2008)	$\alpha = 0$	1.840 20	1.83987	1.80813	1.74779	1.74811	1.49481
		Present	$\alpha = 0$	1.838 16	1.84978	1.83254	1.81938	1.76885	1.49449
			$\alpha = 0.1$	1.92042	1.91731	1.88921	1.82296	1.81310	1.51146
			$\alpha = 0.2$	2.01507	1.99329	1.95185	1.87805	1.85925	1.52903

where $\lambda = m\pi/a$, $\mu = n\pi/b$ and U_{mn}, V_{mn}, W_{bmn}, W_{smn} being arbitrary parameters and ω denotes the Eigen frequency associated with $(m, n)^{\text{th}}$ Eigen mode.

4. Results and discussion

In this section, we present the dynamic analysis of sandwich FGM plate using a new refined shear deformation theory. The effect of the volume fraction of the porosity, power law index, side to thickness ratio and the thickness ratio of the functionally graded layer is studied. In this work, only simply supported boundary conditions are considered. The FG plate is taken to be made of aluminum and alumina with the following material properties:

Ceramic (P_c: Al_2O_3): E_c = 380 GPa; ν = 0.3; ρ_c = 5700 kg/m^3;

Table 3 Fundamental frequency results for perfect and imperfect FGM sandwich plate with FGM core

h/b	Theory	ω				
		α	$k = 1$	$k = 2$	$k = 5$	$k = 10$
0.01	Li *et al.* (2008)	$\alpha = 0$	1.38669	1.44491	1.53143	1.59105
	Present	$\alpha = 0$	1.38666	1.44488	1.53140	1.59103
		$\alpha = 0.1$	1.46163	1.51939	1.60689	1.66791
		$\alpha = 0.2$	1.55024	1.60677	1.69477	1.75715
0.1	Li *et al.* (2008)	$\alpha = 0$	1.34847	1.40828	1.49309	1.54980
	Present	$\alpha = 0$	1.34539	1.40525	1.49055	1.54759
		$\alpha = 0.1$	1.41499	1.47545	1.56209	1.62040
		$\alpha = 0.2$	1.49666	1.55747	1.64520	1.70473
0.2	Li *et al.* (2008)	$\alpha = 0$	1.25338	1.31569	1.39567	1.44540
	Present	$\alpha = 0$	1.24373	1.30615	1.38774	1.43856
		$\alpha = 0.1$	1.30150	1.36650	1.45011	1.50192
		$\alpha = 0.2$	1.36815	1.43643	1.52221	1.57499

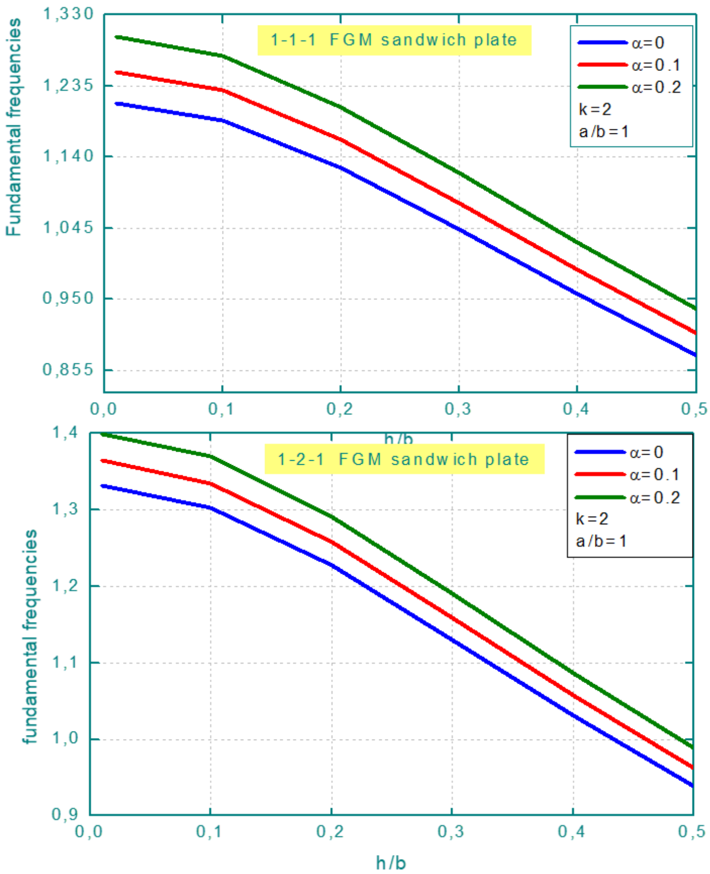

Fig. 3 Porosity influence on the dimensionless frequency versus the thickness ratio h/b for FGM sandwich plate with homogeneous hardcore

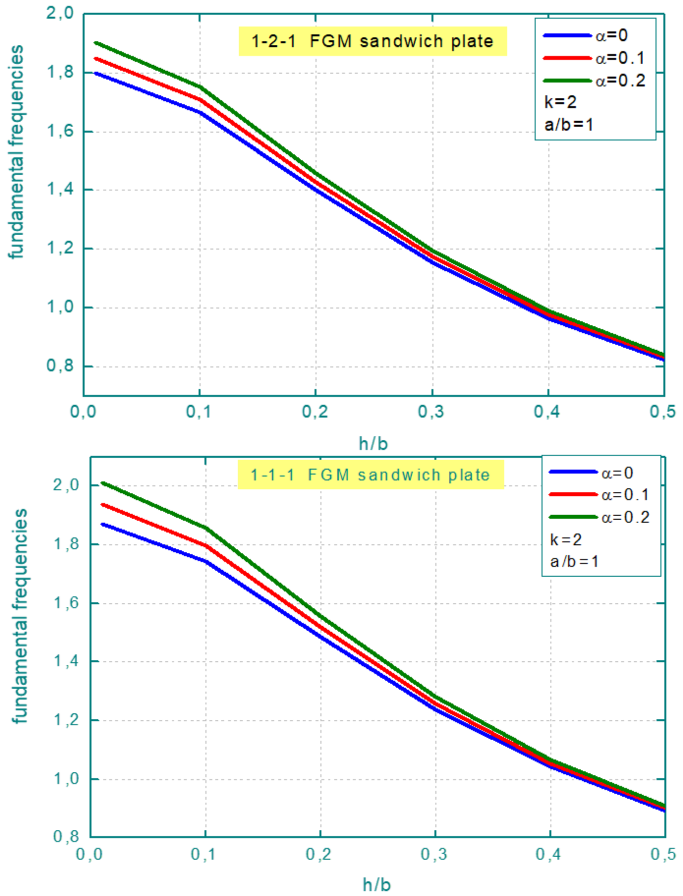

Fig. 4 Porosity influence on the dimensionless frequency versus the thickness ratio *h*/*b* for FGM sandwich plate with homogeneous soft-core

Metal (P_m: Al): E_m = 70 GPa; ν = 0.3; ρ_c = 2702 kg/m^3.

To validate accuracy of the new refined plate theory, the comparisons between the present results and the available results obtained by Li *et al*. (2008). for different values of the gradient index, the side to thickness ratio and the layer thickness ratios. Table 1 present the results of the natural fundamental frequency parameter (ω) of simply supported square FGM plates of Type A with six material distributions and for three values of volume fraction of the porosity (α = 0, α = 0.1, α = 0.2). It can be seen that the results show a satisfied agreement with those obtained by Li *et al*. (2008) when $\alpha = 0$ and becomes higher when $\alpha \neq 0$.

The fundamental frequency results for perfect ($\alpha = 0$) and imperfect ($\alpha \neq 0$) FGM sandwich plate with homogeneous soft-core are presented in Table 2. the fundamental frequency is calculated for different value of the power law index (0, 5 and 10) and side to thickness ratio (*h*/*b* = 0.01 and *h*/*b* = 0.1). It can be seen that, the vibration frequencies obtained when $\alpha \neq 0$ are much higher than those computed when $\alpha = 0$.

From the results presented in Table 3, it is shown that with increase of material rigidity (from 1 to 10) and volume fraction of the porosity (from 0 to 0.2) causes an increase in the fundamental

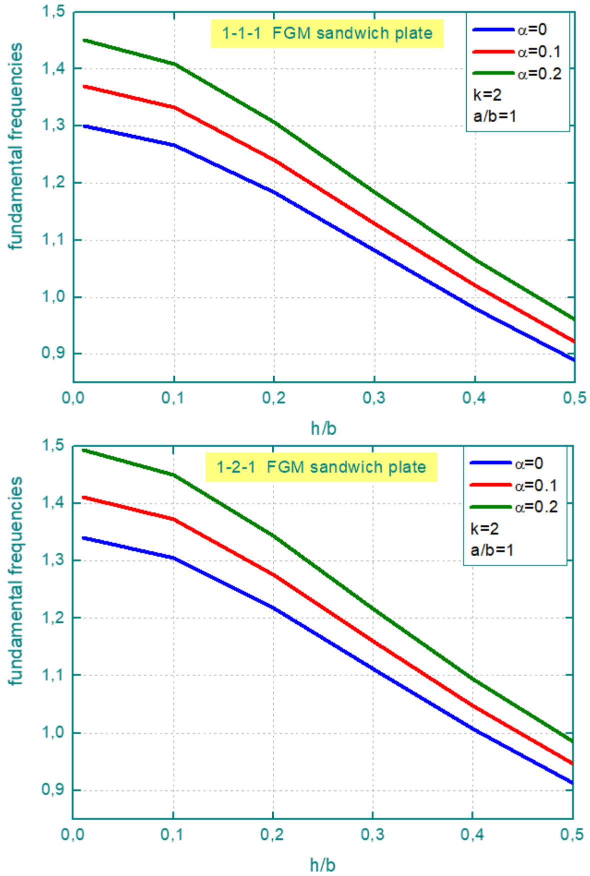

Fig. 5 Porosity influence on the dimensionless frequency versus the thickness ratio *h*/*b* for FGM sandwich plate with FGM core

frequency. This last decrease with the increases of the side of the thickness ratio *h*/*b* (from 0.01 to 0.2).

The effect of the porosity in the dimensionless frequency versus the thickness ratio *h*/*b* for FGM sandwich plate with homogeneous hardcore is presented in Fig. 3. As it can be seen, the presence of the porosity in the FGM sandwich plate with homogeneous hardcore increases the dimensionless frequency. Also, it is seen that the results decrease smoothly as the amount of thickness ratio.

Through thickness variation of dimensionless frequency for FGM sandwich plate with homogeneous soft-core with several values of volume fraction of the porosity is shown in Fig. 4. We can observe that decrease with increases of the thickness ratio. Moreover, the dimensionless frequency in the thin plates are more sensitive than the thick plate to the volume fraction of the porosity.

Fig. 5 depicts the dimensionless frequency versus the thickness-side ratios of simply supported power-law FGM sandwich plates with FGM core for different values of the volume fraction of the porosity. The results are the maximum for the thin plates and the minimum for the thick plates. It can be concluded that the thin plates are slightly more sensitive than the thick plate to the porosity for FGM sandwich plates with FGM core.

5. Conclusions

A new simple sinusoidal for four-variable theory of high order shear and normal deformation theory is developed for functionally graded sandwich plates FGM. The principle of virtual displacements is used to derive the governing equations and boundary conditions. Then, analytical solutions for functionally graded porous square sandwich plates are presented. The inclusions of porosity parameters and exponent of the volume fraction P are investigated. The effects of various parameters, such as thickness ratio, gradient index and volume fraction of porosity on the vibration of FGM ceramic-metal sandwich plates symmetrical are all discussed. The effect of the porosity on the dimensionless frequency analysis of simply supported FG sandwich plates based on the present refined plate theory is investigated analytically in this paper. The modified rule of mixture covering porosity phases is used to describe and approximate material properties of the imperfect FG plates. Accuracy and convergence of this theory was verified by comparing the results obtained with those reported in the literature for the perfect FG plate. The influence of the volume fraction of the porosity on the fundamental frequencies are presented numerical and graphical forms. Parametric studies for varying of the power law index, the side-to-thickness ratio, the layer thickness ratios and the volume fraction of the porosity are also discussed. As well, numerical results of the present high order shear and normal deformation theory is accurate in predicting the dynamic response of non-porous sandwich plates. In addition, the present theory gave control results that can be used to evaluate various plate theories, and also to compare with the results obtained by another solution. From this work, it can be said that the present and simple theory for the resolution of the mechanical behavior of FGM plates sandwich with porosity that presses manufacturing defects.

Acknowledgments

This research was supported by the Algerian Ministry of Higher Education and Scientific Research (MESRS) as part of the grant for the PRFU research project n° A01L02UN140120200002 and by the University of Tiaret, in Algeria.

References

Abdedezak, R., Hassaine Daouadji, T., Benferhat, R. and Adim B. (2018), “Nonlinear analysis of damaged RC beams strengthened with glass fiber reinforced polymer plate under symmetric loads”, *Earthq. Struct.*, **15**(2), 113-122. https://doi.org/10.12989/eas.2018.15.2.113.

Abdelhak, Z., Hadji, L., Khelifa, Z., Hassaine Daouadji, T. and Adda Bedia, E.A. (2016a), “Analysis of buckling response of functionally graded sandwich plates using a refined shear deformation theory”, *Wind Struct.*, **22**(3), 291-305. https://doi.org/10.12989/was.2016.22.3.291.

Abdelhak, Z., Hadji, L., Tahar, D. and Adda Bedia, E.A. (2016b), “Thermal buckling response of functionally graded sandwich plates with clamped boundary conditions”, *Smart Struct. Syst.*, **18**(2), 267-291. https://doi.org/10.12989/sss.2016.18.2.267.

Adim, B. and Hassaine, T. (2016), “Effects of thickness stretching in FGM plates using a quasi-3D higher order shear deformation theory”, *Adv. Mater. Res.*, **5**(4), 223-244. https://doi.org/10.12989/amr.2016.5.4.223.

Adim, B., Hassaine Daouadji, T., Benferhat, R. and Hadji, L. (2016), “An efficient and simple higher order shear deformation theory for bending analysis of composite plates under various boundary conditions”, *Earthq. Struct.*, **11**(1), 63-82. https://doi.org/10.12989/eas.2016.11.1.063.

Adim, B., Hassaine Daouadji, T., Rabahi, A., Benhenni, M., Zidour, M. and Boussad, A. (2018), "Mechanical buckling analysis of hybrid laminated composite plates under different boundary conditions" *Struct. Eng. Mech.*, **66**(6), 761-769. https://doi.org/10.12989/sem.2018.66.6.761.

Atmane, H.A., Tounsi, A. and Bernard, F. (2015), "Effect of thickness stretching and porosity on mechanical response of a functionally graded beams resting on elastic foundations", *Int. J. Mech. Mater.*, **13**(1), 71-84. https://doi.org/10.1007/s10999-015-9318-x.

Belkacem, A., Tahar, H. and Abbes, B. (2016a), "Buckling analysis of anti-symmetric cross-ply laminated composite plates under different boundary conditions", *Int. Appl. Mech.*, **52**(6), 126-141. https://doi.org/10.1007/s10778-016-0787-x.

Belkacem, A., Hassaine Daouadji, T., Abbes, B. and Rabahi, A. (2016b), "Buckling and free vibration analysis of laminated composite plates using an efficient and simple higher order shear deformation theory", *Mech. Ind.*, **17**, 512. https://doi.org/10.1051/meca/2015112.

Benferhat, R., Hassaine Daouadji, T., Said Mansour, M. and Hadji L. (2016a), "Effect of porosity on the bending and free vibration response of functionally graded plates resting on Winkler-Pasternak foundations", *Earthq. Struct.*, **10**(6), 1429-1449. https://doi.org/10.12989/eas.2016.10.6.1429.

Benferhat, R., Daouadji, T.H. and Adim, B. (2016b), "A novel higher order shear deformation theory based on the neutral surface concept of FGM plate under transverse load", *Adv. Mater. Res.*, **5**(2), 107-120. https://doi.org/10.12989/amr.2016.5.2.107.

Benhenni, M.A., Daouadji, T.H., Abbes, B., Adim, B., Li, Y. and Abbes, F. (2018), "Dynamic analysis for anti-symmetric cross-ply and angle-ply laminates for simply supported thick hybrid rectangular plates", *Adv. Mater. Res.*, **7**(2), 83-103. https://doi.org/10.12989/amr.2018.7.2.119.

Benhenni, M.A., Hassaine Daouadji, T., Abbes, B., Abbes, F., Li, Y. and Adim, B. (2019a), "Numerical analysis for free vibration of hybrid laminated composite plates for different boundary conditions", *Struct. Eng. Mech.*, **70**(5), 535-549. https://doi.org/10.12989/sem.2019.70.5.535.

Benhenni, M.A., Adim, B., Daouadji, T.H., Abbès, B., Abbès, F., Li, Y. and Bouzidane, A. (2019b), "A comparison of closed form and finite element solutions for the free vibration of hybrid cross ply laminated plates", *Mech. Compos. Mater.*, **55**(2), 181-194. https://doi.org/10.1007/s11029-019-09803-2.

Daouadji, T.H. and Adim, B. (2016a), "An analytical approach for buckling of functionally graded plates", *Adv. Mater. Res.*, **5**(3), 141-169. https://doi.org/10.12989/amr.2016.5.3.141.

Daouadji, T.H. and Adim, B. (2016b), "Theoretical analysis of composite beams under uniformly distributed load", *Adv. Mater. Res.*, **5**(1), 1-9. https://doi.org/10.12989/amr.2016.5.1.001.

Daouadji, T.H. and Benferhat, R. (2016), "Bending analysis of an imperfect FGM plates under hygro-thermo-mechanical loading with analytical validation", *Adv. Mater. Res.*, **5**(1), 35-53. https://doi.org/10.12989/amr.2016.5.1.035.

Daouadji, H.T., Benyoucef, S., Tounsi, A., Benrahou, K.H. and Bedia, A.E. (2008), "Interfacial stresses concentrations in FRP - damaged RC hybrid beams", *Compos. Interf.*, **15**(4), 425-440. https://doi.org/10.1163/156855408784514702.

Delale, F. and Erdogan, F. (1983), "The crack problem for a nonhomogeneous plane", *J. Appl. Mech.*, **50**(6), 609-614. https://doi.org/10.1115/1.3167098.

Hadji, L., Tahar, D. and Adda Bedia, E.A. (2015), "A refined exponential shear deformation theory for free vibration of FGM beam with porosities", *Geomech. Eng.*, **9**(3), 361-372. https://doi.org/10.12989/gae.2015.9.3.361.

Hadj, B., Rabia, B. and Daouadji, T.H. (2019), "Influence of the distribution shape of porosity on the bending FGM new plate model resting on elastic foundations", *Struct. Eng. Mech.*, **72**(1), 823-832. https://doi.org/10.12989/sem.2019.72.1.061.

Hassaine Daouadji, T. (2013), "Analytical analysis of the interfacial stress in damaged reinforced concrete beams strengthened by bonded composite plates", *Strength Mater.*, **45**(5), 587-597. https://doi.org/10.1007/s11223-013-9496-4.

Hassaine Daouadji, T. (2017), "Analytical and numerical modeling of interfacial stresses in beams bonded with a thin plate", *Adv. Comput. Des.*, **2**(1), 57-69. https://doi.org/10.12989/acd.2017.2.1.057.

Hassaine, D.T., Benferhat, R. and Adim, B. (2016a), "Bending analysis of an imperfect advanced composite plates resting on the elastic foundations", *Coupled Syst. Mech.*, **5**(3), 269-285. https://doi.org/10.12989/csm.2017.5.3.269.

Hassaine Daouadji, T., Rabahi, A., Abbes, B. and Adim, B. (2016b), "Theoretical and finite element studies of interfacial stresses in reinforced concrete beams strengthened by externally FRP laminates plate", *J. Adhes. Sci. Technol.*, **30**(12), 1253-1280. https://doi.org/10.1080/01694243.2016.1140703.

Hassaine Daouadji, T., Chedad, A. and Adim B. (2016c), "Interfacial stresses in RC beam bonded with a functionally graded material plate" *Struct. Eng. Mech.*, **60**(4), 693-705. http://dx.doi.org/10.12989/sem.2016.60.4.693.

Ichikawa, K. (2000) *Functionally Graded Materials in the 21st Century, a Workshop on Trends and Forecasts*, Kluwer Academic Publishers, USA.

Koizumi, M. (1997), "FGM activities in Japan", *Compos. Part B,* **28**(1-2), 1-4. https://doi.org/10.1016/S1359-8368(96)00016-9.

Li, Q., Iu, V.P. and Kou, K.P. (2008), "Three-dimensional vibration analysis of functionally graded material sandwich plates", *J. Sound Vib.*, **311**(112), 498-515. https://doi.org/10.1016/j.jsv.2007.09.018.

Natarajan, S. and Manickam, G. (2012), "Bending and vibration of functionally graded material sandwich plates using an accurate theory", *Finite Elem. Anal. Des.*, **57**, 32-42. https://doi.org/10.1016/j.finel.2012.03.006.

Pradhan, S.C. and Murmu, T. (2009), "Thermo-mechanical vibration of FGM sandwich beam under variable elastic foundations using differential quadrature method", *J. Sound Vib.*, **321**, 342-362. https://doi.org/10.1016/j.jsv.2008.09.018.

Rabahi, A., Hassaine Daouadji, T. and Adim, A. (2016a) "Analytical and numerical solution of the interfacial stress in reinforced-concrete beams reinforced with bonded prestressed composite plate", *J. Reinf. Plast. Compos.*, **35**(3), 258-272. https://doi.org/10.1177/0731684415613633.

Rabia B., Hassaine Daouadji, T. and Mansour, M. (2016b), "Free vibration analysis of FG plates resting on the elastic foundation and based on the neutral surface concept using higher order shear deformation theory", *Comptes Rendus Mecanique,* **344**(9), 631-641. https://doi.org/10.1016/j.crme.2016.03.002.

Rabia, B., Hassaine, D.T., Hadji, L. and Said Mansour, M. (2016c), "Static analysis of the FGM plate with porosities", *Steel Compos. Struct.*, **21**(1), 123-136. https://doi.org/10.12989/scs.2016.21.1.123.

Rabahi, A., Hassaine Daouadji, T., Benferhat R. and Adim B. (2018a), "Elastic analysis of interfacial stress concentrations in CFRP-RC hybrid beams: Effect of creep and shrinkage", *Adv. Mater. Res.*, **6**(3), 257-278. https://doi.org/10.12989/amr.2017.6.3.257.

Rabia, B., Abderezak, R., Daouadji, T.H., Abbes, B., Belkacem, A. and Abbes, F. (2018b), "Analytical analysis of the interfacial shear stress in RC beams strengthened with prestressed exponentially-varying properties plate", *Adv. Mater. Res.*, **7**(1), 29-44. https://doi.org/10.12989/amr.2018.7.1.029.

Rabahi, A., Benferhat, R. and Hassaine Daouadji, T. (2019), "Elastic analysis of interfacial stresses in prestressed PFGM-RC hybrid beams", *Adv. Mater. Res.*, **7**(2), 83-103. https://doi.org/10.12989/amr.2018.7.2.083.

Rabia, B., Daouadji, T.H. and Abderezak, R. (2019), "Effect of distribution shape of the porosity on the interfacial stresses of the FGM beam strengthened with FRP plate", *Earthq. Struct.*, **16**(5), 601-609. https://doi.org/10.12989/eas.2019.16.5.601.

Shi, Z.F. and Chen, Y. (2004), "Functionally graded piezoelectric cantilever beam under load", *Arch. Appl. Mech.*, **74**, 3-4. https://doi.org/10.1007/s00419-004-0346-5.

Wang, Z.X. and Shen, H.S. (2011), "Nonlinear analysis of sandwich plates with FGM face sheets resting on elastic foundations", *Compos. Struct.*, **93**, 2521-2532. https://doi.org/10.1016/j.compstruct.2011.04.014.

Wattanasakulpong, N. and Ungbhakorn, V. (2014), "Linear and nonlinear vibration analysis of elastically restrained ends FGM beams with porosities", *Aerosp. Sci. Technol.*, **32**(1), 111-120. https://doi.org/10.1016/j.ast.2013.12.002.

Zenkour, A.M. and Sobhy, M. (2010), "Thermal buckling of various types of FGM sandwich plates", *Compos. Struct.*, **93**, 93-102.

https://doi.org/10.1016/j.compstruct.2010.06.012.
Zhu, J., Lai, Z., Yin, Z., Jeon, J. and Lee, S. (2000), "Fabrication of ZrO_2-NiCr functionally graded material by powder metallurgy", *Mater*. *Chem*. *Phys*., **68**, 130-135. https://doi.org/10.1016/S0254-0584(00)00355-2.

CC